 doi:10.20944/preprints202203.0238.v1

Article

Developing an extended virtual blade model for efficient numerical modeling of wind and tidal farms

Soheil Radfar [1,*,‡] and Bijan Kinaoush [2,‡]

[1] Department of Civil and Environmental Engineering, Tarbiat Modares University, Tehran, 14115111, Iran; soheil.radfar@modares.ac.ir
[2] Faculty of Civil Engineering, Khaje Nasir Toosi University of Technology; kianuoshbijan68@gmail.com
* Correspondence: soheil.radfar@modares.ac.ir

Abstract: The Virtual Blade Model (VBM) is the implementation of the Blade element model (BEM). This was done by coupling the Blade Element Momentum theory equations to simulate rotor operation with the Reynolds Averaged Navier-Stokes (RANS) equation to simulate rotor wake and the turbulent flow field around it. Exclusion of actual geometry of blades causes lower computational cost (about 10 to 100 times). Also, due to simplifications in the meshing procedure, VBM is easier to set up than the models that consider the actual geometry of blades. One of the main unaddressed limitations of the VBM code was the constraint of modeling up to ten rotor zones within one computational domain. This paper provides a detailed and well-documented general methodology to develop a virtual blade model for simulation of ten-plus turbines within one computational domain to remove the limitation of this widely used and robust code. It is strongly believed that the technical contribution of this paper, combined with the current sky-rocketing advancement of available computational resources and hardware, would open the gates to simulate various engineering problems in the field of aerospace, clean energy, and many more.

Keywords: Virtual Blade Model; Code extension; CFD modeling; Tidal turbine; Wind turbine

1. Introduction

In response to a growing focus on sustainable development and reducing emissions, renewable energy has come into focus. This approach is encouraged and supported by green funds and climate change action [1]. This energy can be derived from a variety of resources, including solar, wind, ocean, biomass, geothermal, hydroelectric, and hydrogen. Wind energy and tidal energy, among others, are estimated to have global energy potentials of 875 and 1.2 PWh/year, respectively [2,3]. Different designs for these turbines have been developed in order to harness this significant potential. In particular, horizontal axis wind turbines (HAWT) and horizontal axis tidal turbines (HATT) have received much attention. Several energy farms have been built at either a small- or commercial scale. Due to the high costs of these types of equipment (Levelized cost of electricity for onshore wind, offshore wind, and tidal energy are 0.039, 0.084, and 0.20 USD/kWh, respectively [3,4]), numerical modeling of their interactions inside energy farms is inevitable in order to ensure the optimal layout and reliable operation.

There are several numerical models for wind and tidal turbines, including the Sliding mesh model (SMM), Rotating reference frame (RRF), Virtual Blade model (VBM), Actuator disc model (ADM), and Momentum sink model (MSM). SMM and RRF are near-field models with the highest level of fidelity. The first simulates a rotating turbine using a sliding mesh interface, while the latter simulates the flow field around turbine blades in a reference frame that rotates at the speed of the turbine rotor [5,6]. VBM is an implementation of the Blade element model (BEM) within ANSYS FLUENT [7]. In VBM, the actual blades are not directly present and, therefore, eliminates the need for high-resolution mesh around the turbine blades [5,8]. The ADM represents the turbine as a momentum sink, and energy [5]. In ADM turbine rotor is modeled as an infinitely thin porous disc [6]. Cross-comparisons between the numerical models are provided in Table 1. MSM is a low fidelity far-field model that is best suited to modeling large arrays of turbines [6]. The MSM simulates the

 doi:10.20944/preprints202203.0238.v1

mechanics of energy extraction by momentum sinks in the momentum equations [6]. A detailed comparative analysis of the numerical techniques used for wind and tidal turbines are provided in [5,9], and [6,10], respectively.

As can be seen in Table 1, the VBM has very acceptable capability in modeling performance, wake, and turbulence of wind and tidal turbines and provides good predictions with significantly lower computational costs. Investigations on HAWTs have shown that the lack of physical blade geometry in VBM reduces meshing time and computational cost by between 10 and 100 times [5,9,10] and therefore, VBM is easier to set up than the models that consider the actual geometry of blades like SMM or MRF. To sum up, the key benefit of VBM is its optimal trade-off of computational cost and wake characterization [11]. Previous studies [5,7] have shown that it can provide good and realistic wake predictions only at a distance of two radii downstream of a turbine. These advantages clearly demonstrate the remarkable capabilities of VBM compared to the blade-resolved methods, making it a viable and efficient tool for modeling interactions between multiple turbines in energy farms (e.g., wind and tidal arrays).

Renewable energy utilization targets will require large-scale farms with multiple devices. So, a computationally cheap tool plays a vital role in developing such energy farms. However, the current version of the VBM code can only model up to ten rotor zones within one computational domain. Hence, modifying the VBM original code for simulation of ten-plus rotor zones to remove its limitations is believed to have a remarkable contribution to the research and development in the field. To achieve this goal, the paper is structured as follows: in Section 2, a comprehensive overview and classification of relevant studies is conducted. Section 3 discusses the concepts and governing equations of the VBM. A step-by-step methodology to modify the original VBM codes is provided in Section 4. In Section 5, the extended VBM codes will be validated. Finally, the discussion and potential future research directions are provided in 6.

Table 1. Comparison of different modeling approaches for wind and tidal turbines [5,6,9,10].

Model	Performance calculation	Near wake characterization	Far wake characterization	Turbulence modeling	Computational cost*
SMM/RRF	very good	very good	very good	good	100
BEM (VBM)	good	acceptable	very good	acceptable	10
ADM	-	poor	acceptable	-	5
MSM	-	-	acceptable	-	2

* 0-100 scale: "100" highest and "0" lowest computational cost

2. Literature review

VBM is widely used to model helicopter blades, wind energy, and tidal energy. A search in SCOPUS and Google Scholar for publications that utilized VBM for numerical simulation of aircraft and wind/tidal turbines returns a total of 41 articles or conference papers released between 2009 and 2021. The number of documents per year is presented in Figure 1. Moreover, As can be seen, most of the papers were published in 2018. A closer look at Figure 1 shows that ten of these studies investigated HAWTs and nine investigated HATTs. Most of which were published in 2017. Nevertheless, it should be noted that there are several theses, dissertations, and reports that used VBM to study HAWTs and HATTs, e.g., [7,12–19]. They are not accounted for in the statistics of the current section.

Preprints (www.preprints.org) | NOT PEER-REVIEWED | Posted: 17 March 2022 doi:10.20944/preprints202203.0238.v1

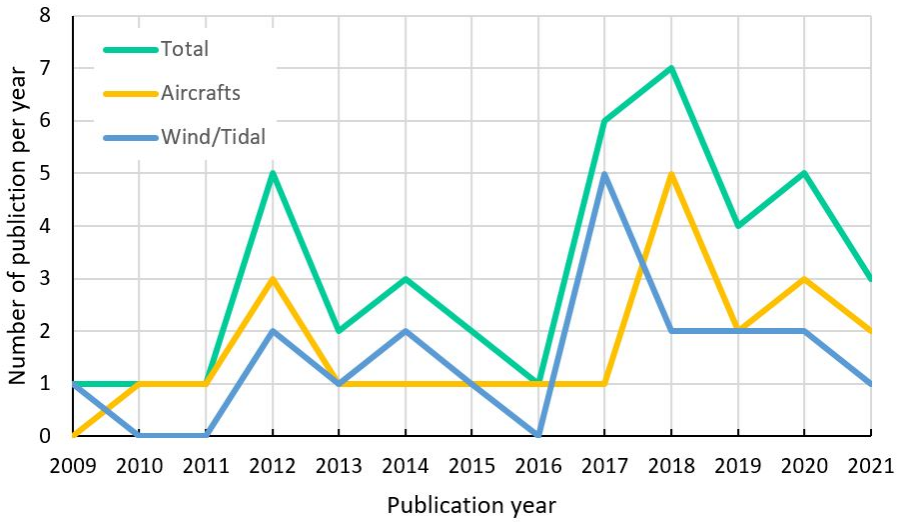

Figure 1. Number of publications that used VBM to numerically simulate turbines and aircrafts.

VBM was originally developed to numerically simulate the performance and turbulent flow field around helicopter rotors. However, later, it was adapted to simulate a single and an array of horizontal axis wind and tidal turbines. Publications on aircrafts cover the impacts of rotating blades using VBM in different types of aircrafts, including helicopter ([20–30]), unmanned aerial vehicle ([31–33]), quad-copter ([34]), turboprop ([35]), and tilt-rotor ([36]). Of which, the helicopter is the most analyzed vehicle (about 60% of all). Also, the number of rotors in these studies ranges from one to four.

Classification of studies on HAWTs/HATTs is provided in Table 2. Studies in the table are presented chronologically, from oldest to the most recent. As can be seen, A large body of research describes the wake characteristics of HAWTs and HATTs. Chick and Makridis [37] studied the wake interactions of two wind turbines at the top of an ideal Gaussian hill. They found that velocity deficits are higher in the flat terrain cases. Nevertheless, after 10D downstream, the maximum velocity deficit increases in complex cases because of the slowing wind speed. Hussein and El-Shishiny [38] investigated onshore micro-scale wind farms consisting of two HAWTs. Makridis and Chick [39] explored the interaction of wind turbine wakes with the terrain. They examined velocity and turbulence at four downstream locations and identified that the maximum wake deficit overprediction was 15% at 4D. Javaherchi et al. [5] simulated the flow field around and in the wake of a HAWT. They compared three models, including RRF, VBM, and ADM, for HAWT performance and wake characterization. Balduzzi et al. [40,41] adapted VBM to analyze rooftop siting of a wind turbine in an urban landscape. Their results showed that a wrong positioning of a HAWT can result in more than 50% performance loss.

Javaherchi et al. [42–44] studied the flow field and energy extraction in a small array of Marine HydroKinetic (MHK) turbines (also referred to as HATT). They found that VBM has limitations to model the turbine performance accurately at very low and high tip speed ratios (TSRs). Nevertheless, it provides a good compromise between cost and accuracy in rather far wake regions. They also employed the same methodology to investigate sediment transport in wake [45]. Sufian et al. [46,47] developed models to simulate the interaction of a HATT and free surface waves. They concluded that this interaction extended wavelength by about 12% and reduced the wave height by about 10%. Later, [8] investigated this effect and reported a reduction of 3% in wave height for a single turbine. Their results suggest a 7% increase in bed stress upstream of the turbine.

Bowman et al. [48] proposed a physics-based actuator disk model (PBADM) for a HATT and compared it with ADM and VBM. They reported that VBM over-predict the wake deficit. Also, it produces the largest amount of transverse velocity. Lombardi et al. [49] explored the effect of blockage and found that the performance of a downstream HATT can increase up to 5% with a lateral spacing of 1.5D. Attene et al. [11] implemented a

 doi:10.20944/preprints202203.0238.v1

methodology to maximize tidal stream turbine power. They found that an optimal lateral spacing of $3D$ between two side turbines in a row increases the turbine power by nearly 20%. Santos et al. [50] studied the wake characteristics and configuration of the HATTs in a river channel and obtained wake lengths between 7 and 9 diameters. Recently, [51] adapted VBM to study an array of HATTs and developed a linear methodology to predict the maximum power output of the turbines based on available kinetic energy flux at 1D upstream of HATTs.

Articles and conference papers focused on HAWTs and HATTs are listed in Table 2. They are classified and organized based on the purpose of each study, number of turbines, turbine model, and turbine dimension. Basically, the VBM methodology was developed and validated for HAWTs and HATTs by taking advantage of the similar underlying physics of these two different engineering technologies. As it is seen in Table 2, the majority of studies simulated a scaled version of turbine designs and a handful number of turbines. This is not in line with the current significant demand for the study and development of energy farms. Overview of literature that relates to HATTs found that far-field models (MSM and Bed roughness model (BRM)) are the most common models to investigate the impacts of turbine arrays [6]. As it was concluded from Table 1, they are low fidelity models unable to capture near wake characteristics and performance of turbines. This motivates the need for a cost-effective and reliable technique to explore wind and tidal arrays. Hence, VBM would be of great interest in this respect. This necessitates the current study to remove the limitation of ten rotors in the original codes of VBM. Another important aspect to note is that "NREL" and "DOE RM1" reference models are the most common benchmark designs for HAWTs and HATTs. Furthermore, almost all studies have been focused on wake characterization (interaction with other turbines, wave, and water surfaces).

 doi:10.20944/preprints202203.0238.v1

Table 2. Classification of studies on wind and tidal turbines using VBM. [5,6,10,52].

Study	Type	Scope	Objective	Number of turbines	Turbine model	Turbine dimension
[37]	CP	HAWT[1]	Wake interaction	2	NREL 5MW	Full
[38]	AR	HAWT	Wake interaction	1, 2	Tjaereborg turbines	Full
[53]	AR	HAWT	Wake interaction	2	NTK 500/41	Full
[39]	AR	HAWT	Wakes with terrain effects	2, 6	Nibe turbines	Full
[42]	AR	HATT	Wake characteristics	1	DOE RM1	Scaled
[5]	AR	HAWT	Wake characteristics	1	NREL Phase VI	Scaled
[46]	CP	HATT[2]	Wake characteristics	1	Wortmann FX 63-137	Scaled
[43]	CP	HATT	Wake characteristics	1	DOE RM1	Scaled
[52]	AR	HAWT	Wake characteristics	1	NREL Phase VI	Scaled
[44]	AR	HATT	Wake characteristics	1	DOE RM1	Scaled
[47]	AR	HATT	Wave and turbine interaction	1	Wortmann FX 63-137	Scaled
[45]	AR	HATT	Sediment transport in wake	1	DOE RM1	Scaled
[40]	AR	HAWT	Wake interaction	1	NREL Phase II	Scaled
[41]	CP	HAWT	Wake interaction	1	NREL Phase II	Scaled
[48]	AR	HATT	Wake characteristics	1	Wortmann FX 63-137	Scaled
[8]	AR	HATT	Wave and turbine interaction	1	Hull University model	Scaled
[11]	AR	HATT	Wake interaction in tidal array	1, 2	IFREMER model	Scaled
[49]	AR	HATT	Effect of the blockage	1, 2	Wortmann FX 63-137	Full, Scaled
[50]	AR	HATT	Wake characteristics	1, 3	Notre Dame turbine	Full

[1] Horizontal Axis Wind Turbine
[2] Horizontal Axis Tidal Turbine

3. Virtual Blade Model (VBM)

In 1995 Zori et al. [54] published a general Computational Fluid Dynamics (CFD) code that greatly yet efficiently simplified numerical modeling approach to simulate a helicopter rotor operation and flow field around it. Later on, the implementation of the published code by Zori. et al. was adapted within ANSYS FLUENT that significantly enhanced its usage and application [55]. The originality of this code lies under the efficient modeling of the helicopter rotor blade shape, with variable profile shape and angles along the blade span, and their effect on the surrounding flow via the Blade Element Momentum theory's (BEMT) equations [56]. The distinction between BEMT and VBM is that the latter incorporates all three components of the RANS momentum equations, while the former uses only a simplified equation [11]. This approach eliminates the requirement of generating, gridding,

Preprints (www.preprints.org) | NOT PEER-REVIEWED | Posted: 17 March 2022 doi:10.20944/preprints202203.0238.v1

and numerically simulating the helicopter rotor blade's complex geometry and flow field and simulating it virtually (i.e., virtual blade model). This exclusion of the actual geometry of blades from numerical modeling of the turbine blades reduces computational costs even up to 100 times while providing an accurate effect of the turbine far wake and turbine-turbine wake interaction [9,16]. As the actual geometry of blades is not directly present in the model, the name Virtual Blade Model (VBM) is used for this rotor representation [5]. The general idea of VBM is that it models the effect of the rotating turbine blades on its surrounding flow field (i.e., rotor wake) via coupling the solution of BEM equations with the Reynolds Averaged Navier-Stokes (RANS) equations. In this respect, the BEM solution is integrated into the RANS equation as external body forces (i.e., by means of source terms in the momentum equations [39]). This process is done iteratively until a converged numerical solution for the rotor operation in the flow field is attained.

In the VBM, turbine blade span is divided into small elements from root to tip (up to 20 sections), and the lift and drag forces of sections are computed based on the local angle of attack (AOA), chord length, and airfoil shape. The lift and drag forces for each section is calculated as follows [7]:

$$f_{L,D} = \frac{1}{2} C_{L,D}(AOA, Ma, Re) \cdot c_{(r/R)} \cdot \rho \cdot A \cdot V_{tot}^3 \tag{1}$$

where $c_{(r/R)}$ is the chord length of the segment and is provided by the manufacturer, ρ is the fluid density, A is the rotor swept area, V_{tot} is the fluid velocity relative to the blade and $C_{L,D}$ are the lift- and drag coefficients come from a lookup table that contains the values as a function of the Mach number (Ma), the Reynolds number (Re) and AOA for the blade airfoils. AOA is defined as follows [13]:

$$AOA = \tan^{-1} \frac{U}{\omega R} \tag{2}$$

where U is the streamwise velocity (i.e., the velocity perpendicular to the plane of rotation), ω is the angular velocity, and R is the radius of the rotor disk. This rotor disk zone is a thin fluid sub-domain with an area equal to the blades' swept area over a complete revolution. It should be noted that the dynamic effect of blades rotation is simulated based on time-averaged body forces over the thin full disk. Accordingly, the lift and drag forces are averaged over a full blade revolution to calculate the forces per cell as follows [14]:

$$F_{L,D_{\text{cell}}} = N_b \cdot \frac{dr \cdot d\theta}{2\pi} \cdot f_{L,D} \tag{3}$$

where N_b is the number of blades, r is the radial position of the blade section from the center of the turbine, θ is the azimuthal coordinate.

This time-averaged force is used to calculate the equivalent source term for each mesh cell. Therefore, the momentum source term for each cell of the numerical discretization is [14]:

$$\vec{S}_{\text{cell}} = -\frac{\vec{F}_{\text{cell}}}{V_{\text{cell}}} \tag{4}$$

where V_{cell} is the volume of the grid cell. These forces are applied to the fluid at each calculation step, and the flow is updated. This iterative process continues until the convergence is reached [13]. As can be seen, VBM indirectly considers the effect of rotating blades through the introduction of momentum source terms that act within the rotor disk zone [49]. A brief description of general steps to implement VBM within ANSYS FLUENT is provided in Appendix A.

Preprints (www.preprints.org) | NOT PEER-REVIEWED | Posted: 17 March 2022 doi:10.20944/preprints202203.0238.v1

4. Methodology

VBM is a set of four User Defined Functions (UDFs) developed in C programming language for use in ANSYS FLUENT. Modifications have been made to simulate ten-plus rotor zones in the original UDF code written in C language. The four UDFs are:

- rotor_model_v10.1.c;
- rotor_model_v10.scm;
- thread_mem_v1.0.c;
- thread_mem.h.

In the current version of the code, modifications have been done to simulate twenty rotor zones. In this regard, the first two UDFs will be updated, and the other two will remain unchanged. Needless to say, it is possible to model infinite rotor zones by employing the present methodology. It is only a matter of understanding where modifications must be made.

4.1. Changes applied to "rotor_model_v10.1.c"

The core calculations are performed through "rotor_model_v10.1.c". This UDF consists of four sections: "Global Input Variables," "Global Trimming Variables," "Global Memory," and "All Functions." The code structure is depicted in Figure 2. Each function has its specific variables and uses some global variables. These global variables play an important role in the calculations of rotor zones and are used by most of the functions. Therefore, they are introduced at the beginning of all functions.

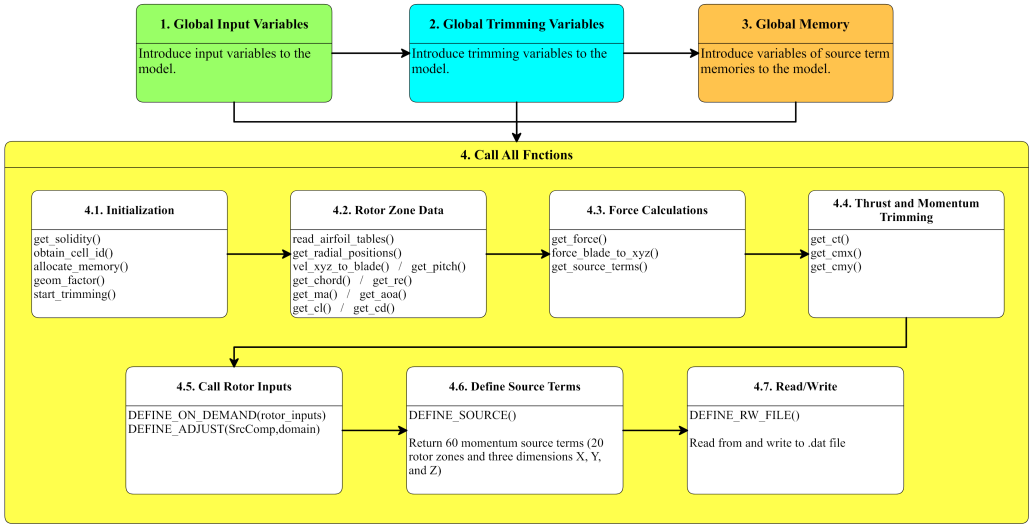

Figure 2. Structure of the main code and its functions.

The first section deals with the global input variables. The first and foremost variable that is utilized is "*nrtz*," which represents the number of rotor zones. The quantity of this variable is introduced via GUI as an integer number. The previous version of the code was limited to ten rotor zones, extended to twenty rotor zones. Following *nrtz*, the code reads settings related to the number of blades, rotor radius, rotor speed, tip effect, rotor disk origin, and angle, blade pitch and flapping, number of blade sections, twist and chord specifications, and lift- and drag coefficients. The number of rotor zones directly influences these variables. It means that the number of rotor zones controls how many times a loop should be executed in a function. So they must be changed and extended to 20. It should be noted that some of these arrays may have more than one dimension (e.g., twist and chord specifications, or lift- and drag coefficients: variables *cin*, *cout*, *csec*, *twst*, and *clorcd*), but only the dimension which is related to the number of rotor zones must be modified. For

Preprints (www.preprints.org) | NOT PEER-REVIEWED | Posted: 17 March 2022 doi:10.20944/preprints202203.0238.v1

most of these variables, it is the first dimension; on the other hand, it is the second or the third for a few of them.

In the next section, trimming variables are provided and should be modified to consider 20 rotor zones. It is worth mentioning that trim variables for soft-in-plane isotropic blade [57]. Nevertheless, they are not applicable for the simulation of horizontal axis wind or tidal turbines and remain disabled in the VBM panel. In the global memory section, the number of rotor cell zone and source terms are introduced to the model. These variables are related to *nrtz*, and extended to 20, accordingly.

In the next step, functions are explored to check their local variables. A few of these functions contain the above-mentioned variables and are related to the number of rotor zones. Therefore, modifications have been made to account for twenty rotor zones. The VBM code outputs are momentum source terms that are in three dimensions. A function in the code is responsible for calculating momentum quantities. Another function, executed at the final stage of the code, returns these quantities to ANSYS FLUENT software. In order to make a connection between these two functions, momentum quantities should be stored in the memory. This memory allocation is executed in the first part of section four. Every single rotor zone has a counter and three momentum quantities. In other words, every rotor zone requires four memory allocations. Since the number of rotor zones has been doubled, the number of these memory allocations has also been modified from ten to twenty in the next step (lines 237-416 in the original code and 237-488 in the modified code).

For large problems with a huge number of cells, the code must run in parallel mode. For this reason, in some parts, data are transmitted from host to node processors and *vice versa*. The number of times the data is transmitted between hosts and nodes is proportional to the number of rotor zones. Consistent with the rest of the modifications, this number has been changed from ten to twenty. These modifications have been applied to lines 2790-2850 of the original code (lines 2862-2922 of the modified code).

The final part of the code consists of functions that return momentum quantities to the RANS solver (here, ANSYS FLUENT). There are three functions, named "DEFINE_SOURCE," for a single rotor zone to return momentum sources in all three directions. For these functions, it is required to add X-Y-Z momentum source terms to account for rotor zones number eleven to twenty. This has been carried out in lines 4199-5018 of the modified code). There are also some other minor modifications highlighted in the difference check of the original and extended codes (it is included as the paper's supplementary material). All in all, as a result of the applied changes, the number of lines of the code has increased from 4239 to 5129.

4.2. Changes applied to "rotor_model_v10.scm"

The function of this file has been written in SCHEME language to enable VBM in the list of available models inside ANSYS FLUENT and input all Rotor parameters through a GUI panel. A modification has been made to this file. In the section "GEOMETRY - Hub - Number of Sections Details" and line 597, 'maximum 10' is replaced by 'maximum 20.' This extends the number of rotor zones from ten to twenty.

5. Numerical results

This section outlines the numerical results to validate the developed model. In order to do this, the new VBM codes are used to simulate two case studies with one and twelve MHK turbines.

5.1. Validation of a single turbine model

The results of previous studies in National Renewable Energy Laboratory (NREL) [58] and Multiphase and Cardiovascular Flow Lab at the University of Washington [59] have been used to validate the developed model for a single turbine case. The general settings and adapted numerical schemes are based on the previous study of the authors ([51,60]) on MHK turbines. In our model, inlet and outlet boundaries are modeled as velocity inlet

 doi:10.20944/preprints202203.0238.v1

and pressure outlet, respectively (see Figure 3). At the inlet boundary, the free stream velocity is 1.9 m/s. Turbine hub is modeled as a no-slip wall and the outer boundaries of the model are slip-free walls. A DOE RM1 is used as a reference model in the present study. This is an open-source design for a horizontal axis hydrokinetic turbine developed in National Renewable Energy Laboratory (NREL), and researchers can use it to benchmark their studies. [58]. This MHK turbine has a diameter (D) of 20 meters, and its rotor speed is 11.5 rpm. To specify the turbulence, the turbulence intensity is 5%, and the length scale is 1 m. The turbulence intensity is defined as the ratio of the root-mean-square of the velocity fluctuations to the mean flow velocity [59]. In turbulent flows, the turbulence length scale describes the size of the large eddies that contain most of the energy. Accordingly, the tip speed ratio (TSR) equals 6.3. TSR is formulated as follows:

$$TSR = \frac{\omega R}{U} \tag{5}$$

To ensure reproducibility and comparability, the blockage ratio used in this study, was 11.11% as in the study by Tessier and Tomasini [59]. Essentially, it is the ratio between the rotor swept area and the inlet boundary area. It should be mentioned that as opposed to the two benchmarks, our CFD model captures the real geometry of the turbine hub. While the hub is modeled as a thin porous zone within the two benchmarks. Results are summarized in Table 3. The extracted power for each rotor is reported by ANSYS FLUENT as an outcome of the VBM model execution. Comparison with benchmark studies on the DOE RM1 in Table 3 demonstrates the quality of the developed VBM model used in this study. Results indicate that the calculated power of high fidelity SRF model in [58] is 504 kW and its difference with our model is $\approx$ 2%, which is very satisfactory and promising.

Table 3. Power comparison between current model and two benchmark models.

Reference study	Model	Software	Mesh type	Calculated power
NREL [58]	SRF	STAR-CCM	Unstructured	504 kW
Tessier and Tomasini [59]	VBM	ANSYS FLUENT	Structured	458 kW
Developed model	VBM	ANSYS FLUENT	Structured	495 kW

5.2. Validation for a tidal farm model

In this section, further validation of the developed model is shown for tidal arrays with twelve turbines (case of ten-plus rotor zones). As discussed earlier, in the present study, the operation of turbines inside a farm is simulated via BEM coupled with RANS. sketch of the computational domain and imposed boundary conditions are presented in Figure 3. It was decided to use this layout of turbines, because the interpretation of the results for the validation of the model would be quite straightforward: if all turbines in a row have the same extracted power, then the developed code is working correctly and will be validated. As seen in Figure 3, the farm has a rectangular cross-section, and its dimensions are $17.5D \times 5.0D \times 1.5D$ with a hub to hub distance of $1.5D$. The uniform stream-wise velocity at the inlet has a magnitude of 1.75 m/s (this velocity is based on the real tidal stream velocity of the selected farm based on the previous study [61]). The surrounding flow is seawater, and its density is 1025 kg/m^3. Inlet and outlet boundaries are modeled as velocity inlet and pressure outlet, respectively. The other walls of the computational domain are modeled as slip-free walls, and as proposed by [42], turbine nacelle is set as a no-slip condition to capture its effect on wake recovery. Mesh is structured in most of the computational domain except for the regions close to the nacelles. The required mesh resolution for a mesh-independent solution in this study is based on the results in [51]. The user should pay attention to avoid duplicate faces in the meshing of the rotor zone. Besides, the mesh must have a full 360 unit circular face as the rotor face.

Preprints (www.preprints.org) | NOT PEER-REVIEWED | Posted: 17 March 2022 doi:10.20944/preprints202203.0238.v1

In his paper, RANS simulation is closed with Shear Stress Transport or SST $\kappa - \omega$ as the turbulent model, where κ is turbulence kinetic energy, and ω is specific dissipation rate [16]. This model is a modification of the original $\kappa - \omega$ to overcome its limitations for capturing the turbulent boundary layer around the blade. SST $\kappa - \omega$ transitions to the $\kappa - \epsilon$ model for better far-field characterization. Turbulence equations are set to be a second-order upwind scheme. The Semi-Implicit Method for Pressure Linked Equations (SIMPLE) algorithm is deployed as a pressure-velocity scheme to solve the RANS equations. Also, discretization of gradient, pressure and momentum for modeling the flow field around turbine blades are "Green-Gauss Node Based," "Second-Order," and "QUICK."

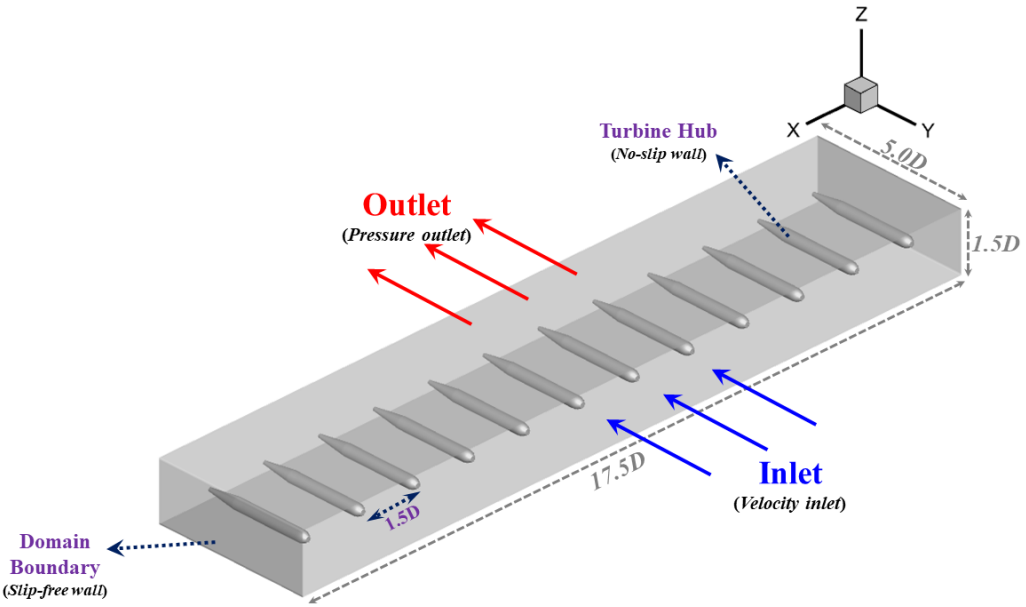

Figure 3. Sketch of the computational domain and boundary conditions.

Figures 4 illustrates the results obtained using the modified VBM codes and above-mentioned numerical settings. They represent the velocity contours in the y–direction for a single row tidal farm with twelve MHK turbines. The velocities are normalized according to the stream-wise velocity at the inlet ($V_y = 1.75$ m/s). The smooth stream-wise velocity contours in this figure support that the model is fully converged. Also, as shown in Figure 4, the flow accelerates around the blades and between turbine nacelles, and as a result, flow velocity increases to $1.3V_{inlet}$. It should be noted that this accelerated flow affects the sedimentation process and is environmentally important. Besides, there is a big velocity deficit behind the blades (or, rotor swept area) because of the extraction of power. Table 4 summarizes the calculated powers of turbines. The results indicate that the total power extracted from this turbines' configuration is 5316 kW. The most significant observation of this validation test is that there is a negligible difference ($\pm 0.02\%$) between the calculated powers of the 12 rotors. As it should be, the extracted powers are almost similar and equal to 443 kW. These results well confirm that the modified code works correctly for 10 to 20 rotors, and the developed methodology can be used reliably to extend the VBM codes and model any desired number of turbines.

Preprints (www.preprints.org) | NOT PEER-REVIEWED | Posted: 17 March 2022 doi:10.20944/preprints202203.0238.v1

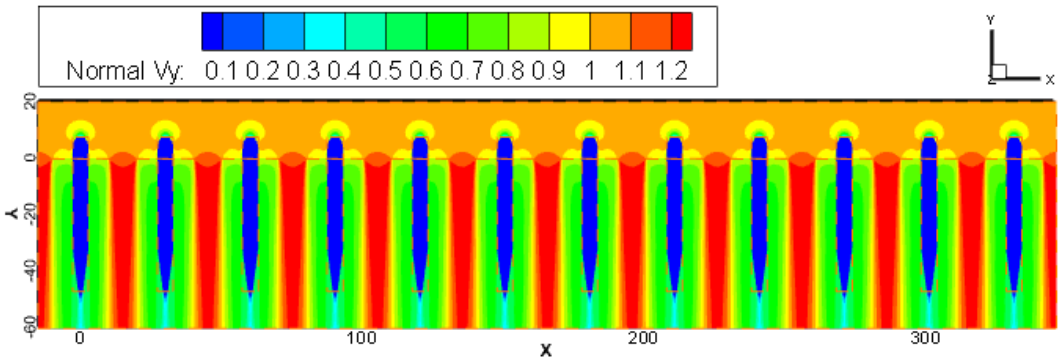

Figure 4. Velocity contours in the y–direction for a single row tidal farm with twelve active rotors.

Table 4. Calculated powers of a single row tidal farm with twelve active.

Rotor No.	R1*	R2	R3	R4	R5	R6	R7	R8	R9	R10	R11	R12
Power [kw]	442.85	443.05	443.05	443.04	443.04	443.04	443.04	443.04	443.05	443.05	443.07	442.94

* The 12 rotors in Figure **??** are numbered from left to right as R1 to R12

6. Discussion

In conclusion, this study demonstrated a methodology to modify UDFs of the virtual blade model (VBM), which is an implementation of BEM within RANS solver (here, ANSYS FLUENT). Good wake and performance representation of VBM, while it provides cost-effectiveness, makes it a very attractive approach to be used in the numerical investigation of wind and tidal turbine arrays. A step-by-step methodology has been provided to update the source codes of VBM and enable it to consider ten-plus rotor zones. The validity and applicability of the modified code have been shown for a single-row array with twelve MHK turbines. Overall the proposed approach can be generalized to any desired number of turbines. It is strongly believed that this detailed and well-documented general methodology would be a significant step toward reliable and efficient modeling of wind and tidal farms. A potential future research direction is to deploy it to study wind and tidal farms with tens of turbines and compare the results with low fidelity far-field models like MSM or BRM.

Author Contributions: "Conceptualization, S.R. and B.K.; Methodology, S.R.; Software, B.K. and S.R.; Validation, S.R.; Formal analysis, B.K. and S.R.; Investigation, S.R. and B.K.; Resources, S.R.; Data curation, S.R.; Writing—original draft preparation, S.R. and B.K.; Review and editing, S.R.; Visualization, S.R.; Supervision, S.R.; Correspondence, S.R. All authors have read and agreed to the published version of the manuscript."

Data Availability Statement: The new developed VBM codes that support the findings of this study are available at https://bitbucket.org/vbm-develop/modified-vbm/src/master/, or upon request from the first author.

Acknowledgments: Authors gratefully acknowledge Dr. Amir Teymour Javaherchi Mozafari for his help and guidance to setup VBM in ANSYS FLUENT.

Conflicts of Interest: The authors declare no conflict of interest.

Abbreviations

The following abbreviations are used in this manuscript:

 doi:10.20944/preprints202203.0238.v1

ADM	Actuator Disc Model
AOA	Angle of Attack
BEM	Blade Element Model
BEMT	Blade Element Momentum theory
BRM	Bed Roughness Model
HATT	Horizontal Axis Tidal Turbines
HAWT	Horizontal Axis Wind Turbines
MHK	Marine Hydrokinetic
MSM	Momentum Sink Model
NREL	National Renewable Energy Laboratory
RANS	Reynolds Averaged Navier-Stokes
RRF	Rotating Reference Frame
SIMPLE	Semi-Implicit Method for Pressure Linked Equations
SMM	Sliding Mesh Model
TSR	Tip Speed Ratio
UDF	User Defined Function
VBM	Virtual Blade Model

Appendix A. General steps to implement VBM inside ANSYS FLUENT

This section provides a brief description of VBM model setup within ANSYS FLUENT. More helpful resources are available at https://nbviewer.org/github/sfo-project/3D-flow-over-WindTidal-turbine-VBM-turbulent/blob/master/Fluent/README.ipynb. General steps to setup the VBM model are as follows:

1. Setup model: According to the physics of the flow field, the user will select the required models to simulate the flow. As mentioned earlier, VBM averages the effect of rotating blades and as a result, in the vast majority of problems it should be run in steady mode. For unsteady implementation, the model UDF should be modified accordingly. In this step, the user downloads the two sources script files "rotor_model_v11.c" and thread_mem_v1.0.c along with the header file thread_mem.h, and then build and load them within ANSYS FLUENT to enable and compile the VBM model. Then, the geometry of rotor (number of sections, radius, chord length and twist degree) will be defined and the model is setup completely.
2. Setup working fluid and solids: The user will provide the physical and thermodynamical properties of the working fluid such as air or water and solids in the problem via the VBM panel. The momentum sources in X, Y and Z directions for each rotor will be defined in this step.
3. Setup boundary and zone conditions: Solving the governing equations of the flow (i.e., system of partial differential equations) requires well-defined boundary conditions within the CFD domain. These conditions are selected and defined in this step.
4. Setup solution methods: In CFD simulations, the governing equations of the flow are solved numerically. Based on the physics of the problem, appropriate "pressure-velocity scheme" and "discretization method for gradient, pressure, momentum and turbulent viscosity" are selected at this step.

References

1. Filom, S.; Radfar, S.; Panahi, R.; Amini, E.; Neshat, M. Exploring wind energy potential as a driver of sustainable development in the southern coasts of iran: The importance of wind speed statistical distribution model. *Sustainability* **2021**, *13*, 7702.
2. Eurek, K.; Sullivan, P.; Gleason, M.; Hettinger, D.; Heimiller, D.; Lopez, A. An improved global wind resource estimate for integrated assessment models. *Energy Economics* **2017**, *64*, 552–567.
3. IRENA. Innovation outlook: Ocean energy technologies. Technical report, International Renewable Energy Agency, Abu Dhabi, UAE, 2020.
4. IRENA. Future of wind: Deployment, investment, technology, grid integration and socio-economic aspects (A Global Energy Transformation paper). Technical report, International Renewable Energy Agency, Abu Dhabi, UAE, October 2019.
5. Javaherchi, T.; Antheaume, S.; Aliseda, A. Hierarchical methodology for the numerical simulation of the flow field around and in the wake of horizontal axis wind turbines: Rotating reference frame, blade element method and actuator disk model. *Wind Engineering* **2014**, *38*, 181–201.

6. Nash, S.; Phoenix, A. A review of the current understanding of the hydro-environmental impacts of energy removal by tidal turbines. *Renewable and Sustainable Energy Reviews* **2017**, *80*, 648–662.
7. Mozafari, A.J. Numerical Modeling of Tidal Turbines: Methodology Development and Potential Physical Environmental Effects. Master's thesis, University of Washington, 2010.
8. Li, X.; Li, M.; Jordan, L.B.; McLelland, S.; Parsons, D.R.; Amoudry, L.O.; Song, Q.; Comerford, L. Modelling impacts of tidal stream turbines on surface waves. *Renewable energy* **2019**, *130*, 725–734.
9. Bianchini, A.; Balduzzi, F.; Gentiluomo, D.; Ferrara, G.; Ferrari, L. Comparative analysis of different numerical techniques to analyze the wake of a wind turbine. In Proceedings of the Turbo Expo: Power for Land, Sea, and Air. American Society of Mechanical Engineers, 2017, Vol. 50961, p. V009T49A017.
10. Masters, I.; Williams, A.; Croft, T.N.; Togneri, M.; Edmunds, M.; Zangiabadi, E.; Fairley, I.; Karunarathna, H. A comparison of numerical modelling techniques for tidal stream turbine analysis. *Energies* **2015**, *8*, 7833–7853.
11. Attene, F.; Balduzzi, F.; Bianchini, A.; Campobasso, M.S. Using Experimentally Validated Navier-Stokes CFD to Minimize Tidal Stream Turbine Power Losses Due to Wake/Turbine Interactions. *Sustainability* **2020**, *12*, 8768.
12. Gosset, A.; Flouriot, G. Optimization of power extraction in an array of marine hydrokinetic turbines. Technical report, Technical report, French Naval Academy, 2008.
13. Cerisola, A. Numerical analysis of tidal turbines using virtual blade model and single rotating reference frame. *Department of Mechanical Engineering-University of Washington, Seattle (WA)-USA: IRENAV, ARTS ET METIERS ParisTech* **2012**.
14. Chen, Z. Analyzing wind turbine wakes with virtual blade model technology using openfoam. PhD thesis, Texas Tech University, 2013.
15. Adamski, S.J. Numerical modeling of the effects of a free surface on the operating characteristics of marine hydrokinetic turbines. PhD thesis, University of Washington, 2013.
16. Javaherchi Mozafari, A.T. Numerical investigation of Marine Hydrokinetic Turbines: methodology development for single turbine and small array simulation, and application to flume and full-scale reference models. PhD thesis, University of Washington, 2014.
17. Hoseyni Chime, A. Analysis of hydrokinetic turbines in open channel flows. PhD thesis, University of Washington, 2014.
18. Li, X. Three-dimensional modelling of tidal stream energy extraction for impact assessment. PhD thesis, The University of Liverpool, UK, 2016.
19. Sufian, S.F. Numerical Modelling of Impacts from Horizontal Axis Tidal Turbines. PhD thesis, The University of Liverpool, UK, 2016.
20. McAlpine, J.D.; Koracin, D.R.; Boyle, D.P.; Gillies, J.A.; McDonald, E.V. Development of a rotorcraft dust-emission parameterization using a CFD model. *Environmental fluid mechanics* **2010**, *10*, 691–710.
21. Pandey, K.; Kumar, U.; Kumar, G.; Deka, D.; Das, D.; Surana, A. CFD Analysis of an Isolated Main Helicopter Rotor for a Hovering Flight at Varying RPM. In Proceedings of the ASME International Mechanical Engineering Congress and Exposition. American Society of Mechanical Engineers, 2012, Vol. 45172, pp. 543–551.
22. Stalewski, W.; Żółtak, J. Optimisation of the helicopter fuselage with simulation of main and tail rotor influence. In Proceedings of the Proceedings of the ICAS Congress, 2012, pp. 2012–1.
23. Bernardo, P.; Mac Réamoinn, R.; Cardiff, P.; Keenahan, J.; Young, P. CFD Modelling of Helicopter Downwash and Assessment of its impact on Pedestrian Comfort. In Proceedings of the The 2018 Civil Engineering Research in Ireland Conference (CERI 2018), University College Dublin, 29-30 August 2018, 2018.
24. Stalewski, W. Simulation and optimization of control of selected phases of gyroplane flight. *Computation* **2018**, *6*, 16.
25. Żółtak, J. Multi-objective and multi-disciplinary design using evolutionary methods applied to aerospace design problems. *Proceedings of the Institution of Mechanical Engineers, Part G: Journal of Aerospace Engineering* **2018**, *232*, 613–625.
26. Kusyumov, A.; Kusyumov, S.; Mikhailov, S.; Romanova, E.; Phayzullin, K.; Lopatin, E.; Barakos, G. Main rotor-body action for virtual blades model. In Proceedings of the EPJ Web of Conferences. EDP Sciences, 2018, Vol. 180, p. 02050.
27. Bernardo, P.; Réamoinn, R.M.; Young, P.; Brennan, D.; Cardiff, P.; Keenahan, J. Investigation of the helicopter downwash effect on pedestrian comfort using CFD. *Infrastructure Asset Management* **2019**, pp. 1–8.
28. Stajuda, M.; Obidowski, D.; Karczewski, M.; Jóźwik, K. Modified virtual blade method for propeller modelling. *Mechanics and Mechanical Engineering* **2020**, *22*, 603–618.
29. Stalewski, W.; Surmacz, K. Investigations of the vortex ring state on a helicopter main rotor using the URANS solver. *Aircraft Engineering and Aerospace Technology* **2020**.
30. Linton, D.; Widjaja, R.; Thornber, B. Actuator Surface Model with Computational-Fluid-Dynamics-Convected Wake Model for Rotorcraft Applications. *AIAA Journal* **2021**, pp. 1–15.
31. Hosseini, Z.; Ramirez-Serrano, A.; Martinuzzi, R.J. Ground/wall effects on a tilting ducted fan. *International Journal of Micro Air Vehicles* **2011**, *3*, 119–141.
32. Tran, D.K.K.; Nguyen, K.; Le, T.H.H.; Nguyen, N.H. Numerical Simulation for The Forward Flight of the Tri-copter Using Virtual Blade Model. *Journal of Advanced Research in Fluid Mechanics and Thermal Sciences* **2020**, *67*, 1–32.
33. Wang, C.H.J.; Nathanael, J.C.; Ng, E.M.; Ng, B.F.; Low, K.H. Framework for the Estimation of Safe Wake Separation Distance between Same-Track Multi-Rotor UAS. In Proceedings of the AIAA Scitech 2021 Forum, 2021, p. 0708.
34. Imam, A.; Bicker, R. Effects of propeller blade twist on reconnaissance quad-rotor UAV. In Proceedings of the The International Conference on Applied Mechanics and Mechanical Engineering. Military Technical College, 2012, Vol. 15, pp. 1–15.

35. Ruiz-Calavera, L.; Funes-Sebastian, D.; Perdones-Diaz, D. Powered model wind tunnel tests of a high-offset subsonic turboprop air intake. In Proceedings of the 46th AIAA/ASME/SAE/ASEE Joint Propulsion Conference & Exhibit, 2013, p. 6502.
36. Li, P.; Zhao, Q.; Zhu, Q. CFD calculations on the unsteady aerodynamic characteristics of a tilt-rotor in a conversion mode. *Chinese Journal of Aeronautics* **2015**, *28*, 1593–1605.
37. Chick, J.; Makridis, A. CFD Modeling of the Wake Interactions of Two Wind Turbines on a Gaussian Hill. *CFD Modeling of the Wake Interactions of Two Wind Turbines on a Gaussian Hill* **2009**, pp. 1000–1004.
38. Hussein, A.S.; El-Shishiny, H.E. Modeling and simulation of micro-scale wind farms using high performance computing. *International Journal of Computational Methods* **2012**, *9*, 1240025.
39. Makridis, A.; Chick, J. Validation of a CFD model of wind turbine wakes with terrain effects. *Journal of wind engineering and industrial aerodynamics* **2013**, *123*, 12–29.
40. Balduzzi, F.; Bianchini, A.; Gentiluomo, D.; Ferrara, G.; Ferrari, L. Rooftop siting of a small wind turbine using a hybrid BEM-CFD model. In Proceedings of the Research and Innovation on Wind Energy on Exploitation in Urban Environment Colloquium. Springer, 2017, pp. 91–112.
41. Balduzzi, F.; Bigalli, S.; Bianchini, A. A hybrid BEM-CFD model for effective numerical siting analyses of wind turbines in the urban environment. In Proceedings of the Journal of Physics: Conference Series. IOP Publishing, 2018, Vol. 1037, p. 072029.
42. Javaherchi, T.; Stelzenmuller, N.; Seydel, J.; Aliseda, A. Experimental and numerical analysis of a scale–model horizontal axis hydrokinetic turbine. In Proceedings of the Proceedings of the 2nd Marine Energy Technology Symposium, Seattle, WA, USA, April 15-18, 2014,.
43. Javaherchi, T.; Stelzenmuller, N.; Aliseda, A. Experimental and numerical analysis of a small array of 45: 1 scale horizontal axis hydrokinetic turbines based on the DOE reference model. In Proceedings of the Proceedings of the 3rd Marine Energy Technology Symposium, Washington, DC, USA, 2015, Vol. 27.
44. Javaherchi, T.; Stelzenmuller, N.; Aliseda, A. Experimental and numerical analysis of the performance and wake of a scale–model horizontal axis marine hydrokinetic turbine. *Journal of Renewable and Sustainable Energy* **2017**, *9*, 044504.
45. Javaherchi, T.; Aliseda, A. The transport of suspended sediment in the wake of a marine hydrokinetic turbine: Simulations via a validated Discrete Random Walk (DRW) model. *Ocean Engineering* **2017**, *129*, 529–537.
46. Sufian, S.F.; Li, M. 3D-CFD Numerical Modeling of Impacts From Horizontal Axis Tidal Turbines in The Near Region. *Coastal Engineering Proceedings* **2014**, pp. 30–30.
47. Sufian, S.F.; Li, M.; O'Connor, B.A. 3D modelling of impacts from waves on tidal turbine wake characteristics and energy output. *Renewable energy* **2017**, *114*, 308–322.
48. Bowman, J.; Bhushan, S.; Thompson, D.S.; O'Doherty, D.; O'Doherty, T.; Mason-Jones, A. A Physics-Based Actuator Disk Model for Hydrokinetic Turbines. In Proceedings of the 2018 Fluid Dynamics Conference, 2018, p. 3227.
49. Lombardi, N.; Ordonez-Sanchez, S.; Zanforlin, S.; Johnstone, C.; et al. A hybrid BEM-CFD virtual blade model to predict interactions between tidal stream turbines under wave conditions. *Journal of Marine Science and Engineering* **2020**, *8*, 969.
50. dos Santos, I.F.S.; Camacho, R.G.R.; Tiago Filho, G.L. Study of the wake characteristics and turbines configuration of a hydrokinetic farm in an Amazonian river using experimental data and CFD tools. *Journal of Cleaner Production* **2021**, *299*, 126881.
51. Radfar, S.; Panahi, R.; Nezhad, M.M.; Neshat, M. A Numerical methodology to predict the maximum power output of tidal stream arrays. *Sustainability* **2022**, *14*, 1664.
52. Bianchini, A.; Balduzzi, F.; Gentiluomo, D.; Ferrara, G.; Ferrari, L. Potential of the Virtual Blade Model in the analysis of wind turbine wakes using wind tunnel blind tests. *Energy Procedia* **2017**, *126*, 573–580.
53. Chen, Z.X.; Marathe, N.; Parameswaran, S. CFD Study of Wake Interaction of Two Wind Turbines. In Proceedings of the Advanced Materials Research. Trans Tech Publ, 2012, Vol. 472, pp. 2726–2730.
54. Zori, L.A.; Rajagopalan, R.G. Navier—Stokes Calculations of Rotor—Airframe Interaction in Forward Flight. *Journal of the American Helicopter Society* **1995**, *40*, 57–67.
55. Ruith, M. Unstructured, multiplex rotor source model with thrust and moment trimming-Fluent's VBM model. In Proceedings of the 23rd AIAA applied aerodynamics conference, 2005, p. 5217.
56. Burton, T.; Jenkins, N.; Sharpe, D.; Bossanyi, E. *Wind energy handbook*; John Wiley & Sons, 2011.
57. Yuan, K.; Friedmann, P.P. Aeroelasticity and structural optimization of composite helicopter rotor blades with swept tips. Technical report, NASA, 1995.
58. Lawson, M.J.; Li, Y.; Sale, D.C. Development and verification of a computational fluid dynamics model of a horizontal-axis tidal current turbine. In Proceedings of the International Conference on Offshore Mechanics and Arctic Engineering, 2011, Vol. 44373, pp. 711–720.
59. Tessier, M.; Tomasini, N. Numerical study of horizontal axis hydrokinetic turbines: performance analysis and array optimization. Technical report, Department of mechanical engineering, University of Washington – Seattle (WA), USA, 2010.
60. Radfar, S. Parametric Study of Turbines Layout Effect on Tidal Energy Farms. Master's thesis, Tarbiat Modares University, 2016.
61. Radfar, S.; Panahi, R.; Javaherchi, T.; Filom, S.; Mazyaki, A.R. A comprehensive insight into tidal stream energy farms in Iran. *Renewable and Sustainable Energy Reviews* **2017**, *79*, 323–338.